Structural, electrical, and optical properties of carbon nanotube-incorporated Al-doped zinc oxide thin films prepared by sol-gel method

Fang-Hsing Wang[1], Ching-Tien Chou[1], Tsung-Kuei Kang[2] and Chia-Cheng Huang[1],
Han-Wen Liu[1] and Chung-Yuan Kung[1]

[1]*Department of Electrical Engineering and Graduate Institute of Optoelectronic Engineering, National Chung Hsing University, Taichung 402, Taiwan*
[2]*Department of Electronic Engineering, Feng Chia University, Taichung 407, Taiwan*

Aluminum-doped zinc oxide (AZO) thin films incorporated with multi-walled carbon nanotubes (MWCNTs) have been prepared by sol-gel technique on glass substrates. The ratio of the MWCNT in sol-gel solution ranges from 0.01 to 1.0 wt.%. This study investigates the effects of MWCNT ratio on structural, electrical, and optical properties of AZO:MWCNT thin films. The XRD analysis showed a strong (0 0 2) peak along the c axis at $2\theta \sim 34.4$ º indicating a hexagonal wurtzite structure for the AZO:MWCNT thin films. The intensity of (0 0 2) peak decreased with the increasing MWCNT ratio, revealing that AZO were bounding with the MWCNTs. The sheet resistance of AZO:MWCNT thin films significantly decreased from 1.38×10^4 to $10.5 \ \Omega/\square$ with increasing the MWCNT ratio from 0.01 to 1.0 wt.%; meanwhile, the optical transmittance in the visible wavelength region decreased from 87.9% to 12.1%, respectively. The figure of merit showed that the developed AZO:MWCNT thin film with the MWCNT ratio of 0.01 wt.% has the optimal electro-optical properties for transparent conducting electrode applications.

Key words: Transparent conducting oxide (TCO), Zinc oxide (ZnO), Carbon nanotube (CNT), Sol-gel, Spin coating.

Introduction

High optical transmittance and low sheet resistance are attractive properties for producing transparent conducting thin films in the application of flat panel displays, touch panels, and solar cells [1-3]. The most utilized material for transparent conductive films is indium tin oxide (ITO) due to its low sheet resistance and high optical transmittance [4]. However, there are some major problems with using ITO films in further applications, such as the inflexibility and insufficiency of rare metals. Carbon nanotubes (CNTs) [5] and aluminum-doped zinc oxide (AZO) [6, 7] have been widely investigated to replace ITO as a new potential material for transparent conductive films. Many methods have been developed to fabricate multi-walled carbon nanotube (MWCNT) films, such as sol-gel method [8-10], air brushing [11], filtration [12, 13] and spraying coating method [14, 15]. Among them, the sol-gel technique offers the possibility of coating of films at a low cost for technological applications. The main challenge, preparing high performance composites, is the homogenous incorporation of CNTs into the matrix material.

In this paper, AZO thin films incorporated with MWCNTs have been prepared by sol-gel technique on glass substrates [16]. The ratio of MWCNT to AZO thin film

varied from 0.01 wt.% to 1.0 wt.%. The structural, electrical, and optical properties of the AZO:MWCNT composite thin film were studied.

Experiment

AZO sol-gel solution was prepared by putting zinc acetate and aluminum chloride (MERCK Ltd.) powder into ethanolamine (MERCK Ltd.) and ethylene glycol monomethyl ether (MERCK Ltd.) solution. The aluminum content in the composite solution was 1.0 at.%. After that, the composite solution was heated to 80 ºC, stirred for 1 h and then stewed for 48 h at room temperature. Finally, the MWCNTs (Golden Innovation Business Co., Ltd, 95% purity) with different ratios from 0.01 wt.% to 1.0 wt.% and surfactant (PVP K30) were added into the solution and then the mixed solution was dispersed by sonicator for 60 min.

Glass substrates (Corning 1737) were cleaned by ethanol, acetone, and D.I. water and then dried in nitrogen. First, the substrates were pre-rotated with 700 rpm and 3000 rpm for 10 s each in a spin coater. Then the AZO:MWCNT composite solution was dribbled on the substrate and subsequently the substrate was rotated with 700 rpm and 3000 rpm for 10 s and 30 s, respectively. Then the substrate was baked at 350 ºC for 10 min to remove organic residuals. These spin-coating steps were repeated for 5 times to keep the thin film thickness of about 150 nm. These thin films were finally annealed in ambient of Ar and H_2 at 450 ºC for 1 h.

*Corresponding author: Fang-Hsing Wang
Tel : +886-4-22851549 ext.706
Fax: +886-4-22851410
E-mail: fansen@dragon.nchu.edu.tw

The structural properties of thin films were investigated by X-ray diffraction (XRD) (PANalytical, 18 kW rotating anode X-ray generator, Japan) with Cu-Kα radiation (λ = 0.154056 nm) in θ-2θ scan mode and field emission scanning electron microscopy (FE-SEM) (JEOL JSM-6700F, Japan). The electrical and optical properties were measured by four point probe (Napson, RT-70/RG-5, Japan) and a UV-VIS (JASCO, V-570, Japan) spectrometer, respectively.

Results and discussion

Fig. 1 shows the XRD spectra of the AZO:MWCNT thin films with various MWCNT ratios. As the MWCNT ratio varied within 0-0.3 wt.%, all the films exhibit an obvious (0 0 2) preferential orientation at the 2θ position of about 34.4 ° along the c axis perpendicular to the substrate surface, indicating a typical hexagonal wurtzite structure. There is no carbon peak in the XRD spectra. When the MWCNT ratio increased to 1.0 wt.%, a carbon (0 0 2) peak was found at 2θ = 26.4 ° and the ZnO peaks weakened. Besides, the AZO: MWCNT thin films with a lower MWCNT ratio exhibited a higher (0 0 2) peak intensity, revealing that much MWCNTs incorporated in the composite film deteriorated the crystallinity of the AZO thin films. This might be due to MWCNT incorporation and other organic binder [17]. The full-width at half-maximum (FWHM), as Fig. 2 showed, increased with the MWCNT ratio, indicating that the crystallite size of the AZO: MWCNT thin film decreased from 21.3 to 15.5 nm as the MWCNT ratio increased from 0 to 0.3 wt.%.

Table 1 shows the parameters of the XRD patterns shown in Fig. 1. The crystalline plane distance (d) was estimated according to the Bragg formula: λ = 2dsinθ, where λ is the X-ray wavelength (0.154056 nm) and θ is the diffraction angle of the (0 0 2) peak. The lattice constant, c, is equal to 2d for the (0 0 2) diffraction peak. The strain (ε) of the films along c-axis is given by the equation: $\varepsilon = [(c_{film}-c_{bulk})/c_{bulk}]$.

Fig. 3(a-d) shows the cross-section and surface morphology of the AZO:MWCNT composite thin films with the MWCNT ratios of 0, 0.01, and 0.1 wt.%. The cross-section image (Fig. 3(a)) proves the film thickness being about 150 nm. The pure AZO thin film without MWCNT incorporation exhibited a smooth and flat surface, as Fig. 3(b) showed. When the MWCNT ratio
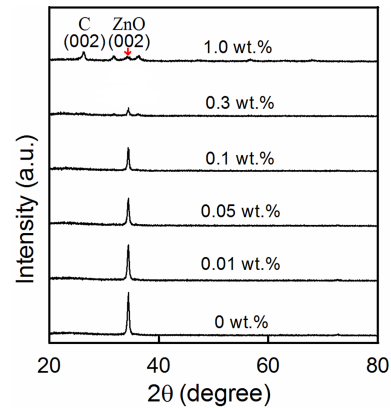

Fig. 1. XRD spectra of the AZO:MWCNT thin films with various MWCNT ratios.
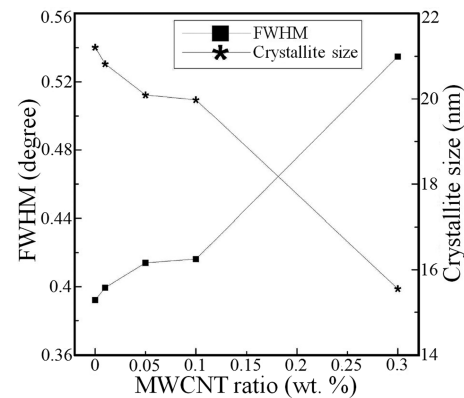

Fig. 2. FWHM and crystallite size of the AZO:MWCNT thin films as a function of MWCNT ratio.

increased to 0.01 wt.%, a little MWCNTs were found to insert in the composite thin film (Fig. 3(c)). Fig. 3(d) shows the surface morphology of the 0.1 wt.% MWCNT sample. The image exhibited that individual MWCNTs were randomly distributed, forming a uniform network. It was also found that some surfactant particles were coated on the MWCNTs. The diameters of MWCNT bundles ranged from 10 to 20 nm. The previous report indicated that well-dispersed CNTs could achieved high electrical conductivity in the MWCNT network because MWCNTs with smaller bundle size provide a larger number of pathways for charge transport [18].

Fig. 4 shows the sheet resistance of AZO:MWCNT thin films as a function of MWCNT ratio. The result showed that the sheet resistance decreased with the

Table 1. The parameters of the AZO:MWCNT films calculated from the XRD patterns.

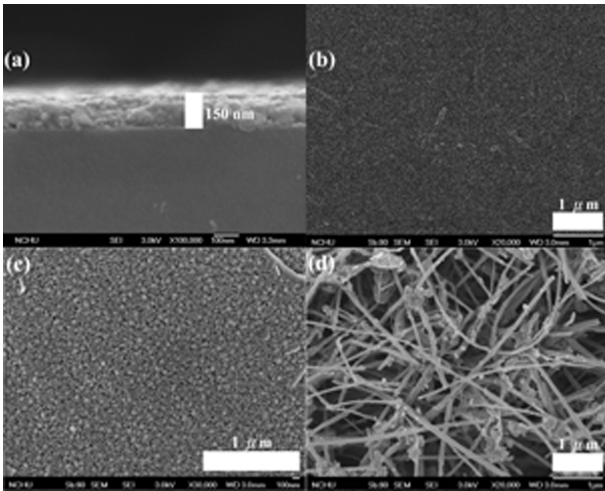| CNT ratio (wt.%)	grain size (nm)	2θ (degree)	FWHM	d (nm)	c (nm)	Strain
0	21.21	34.463	0.39214	0.26002	0.52004	-1.211×10^{-3}
0.01	20.82	34.461	0.39949	0.26004	0.52008	-1.134×10^{-3}
0.05	20.09	34.479	0.41401	0.25991	0.51982	-1.634×10^{-3}
0.1	19.98	34.456	0.41631	0.26008	0.52016	-9.806×10^{-3}
0.3	15.55	34.481	0.53481	0.25989	0.51978	-1.710×10^{-3}

Fig. 3. Cross-section (a) and surface morphology (b)-(d) of the AZO : MWCNT thin films with the MWCNT ratio of 0, 0.01, and 0.1 wt.%.
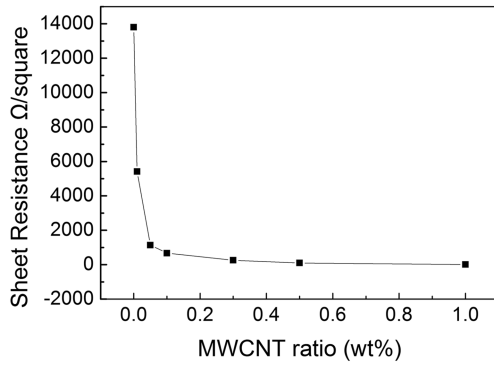

Fig. 5. Optical transmittances of AZO:MWCNT thin films with different MWCNT ratios.

Fig. 4. Sheet resistance of AZO:MWCNT thin films as a function of MWCNT ratio.

Fig. 6. Plot of (αhν)^2 against hν for the AZO:MWCNT thin films with different MWCNT ratios.

increasing MWCNT ratio. Liu et al. [5] and Lee et al. [6] have reported that CNT type and ratio can influence the film conductivity. The sheet resistance significantly decreased from over 10^4 to 10.5 Ω/□ when the MWCNT ratio increased from 0 to 1.0 wt.%. It is believed that enough well-dispersed MWCNTs incorporated in the thin film may form a conducting network to enhance the film conductivity.

Fig. 5 shows the optical transmittances of AZO thin films incorporated with different MWCNT ratios. For transmittance measurement, the thin films were irradiated at a perpendicular angle of incidence with a glass being the reference. The average transmittances in the visible wavelength region (400-700 nm) were 88.5%, 85.5%, 74.6%, 64.5, and 12.1% for the MWCNT ratio of 0, 0.01, 0.05, 0.1 and 1.0 wt.%, respectively. The considerably decreased transmittance with the increasing MWCNT ratio is due to that CNTs tend to absorb visible light. In addition, all the thin films exhibited a sharp absorption edge in the ultraviolet region due to the onset of fundamental absorption of ZnO.

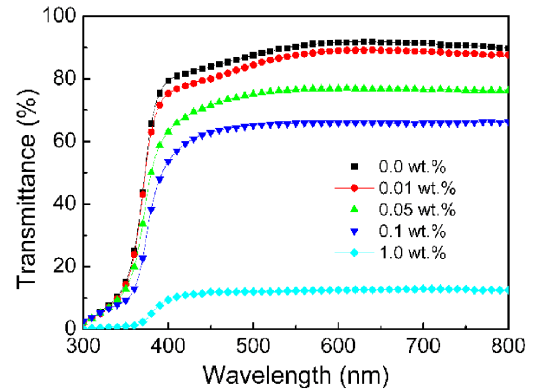The optical absorption coefficient, α, can be calculated from the relation [19]:

$$T = (1-R)^2 \exp(-\alpha d) \qquad (1)$$

where T and R are the transmittance and reflectance of films, and d is the film thickness. In the direct transition semiconductor, α and the optical energy bandgap (E_g) are related by

$$(\alpha h\nu)^2 = A(h\nu - E_g), \qquad (2)$$

where h is Planck's constant, A is a constant and ν is the frequency of the incident photon. Dependence of (αhν)^2 on photon energy (hν) was examined to determine optical bandgap energy (E_g) of the AZO:MWCNT thin film. Fig. 6 shows the plot of (αhν)^2 against hν to obtain E_g of the films, and the E_g can be accurately determined by the extrapolation of the linear regions on the energy axis [20]. The optical bandgap of the AZO:MWCNT thin film first widened for MWCNT ratio of 0.01 wt.% and then narrowed for a further increase in the MWCNT ratio. The variation in the optical bandgap, known as the Burstein-Moss effect, pointed out that E_g would increase with increasing carrier concentration [21].

Fig. 7 exhibits the figures of merit for the AZO: MWCNT thin films with various MWCNT ratios. The
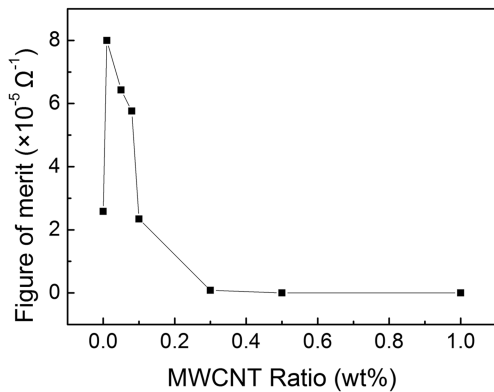
Fig. 7. Figures of merit for the AZO : MWCNT thin films with various MWCNT ratios.

Table 2. Weight percentages of different elements in different ratios of AZO:MWCNT films.

	C (at.%)	O (at.%)	Al (at.%)	Zn (at.%)
0 wt.%	8.52	44.95	11.16	35.37
0.05 wt.%	11.22	38.01	8.84	41.94
0.1 wt.%	27.77	24.64	3.57	44.02

figure of merit (FOM) defined by Haacke [22] equals T^{10}/R_S, providing a way for evaluating the opto-electrical properties of TCO films. T is the average optical transmittance and R_S is the sheet resistance. The result showed that the thin films with MWCNT ratio of 0.01-0.08 wt.% yielded larger FOM than the pure AZO thin film. The highest FOM of $8.0 \times 10^{-5}\ \Omega^{-1}$ was obtained for the film with 0.01 wt.% MWCNTs. This result indicates that appropriate MWCNTs incorporated in AZO thin films can effectively improve opto-electrical properties of AZO thin films.

The changes of element percentages for MWCNTs with different ratios of MWCNTs were analyzed with an energy dispersive spectrometer (EDS) associated with the SEM system. The results are shown in Table 2, which indicated that the significant increase of C resulting from the increase of the MWCNT ratio. Note that H can't be detected by EDS element analysis equipment due to its low atomic weight. And the C had been detected at 0 wt.%-AZO:MWCNT thin films was from the ethanolamine and ethylene glycol monomethyl ether.

Conclusions

The structural, electrical, and optical properties of the AZO:MWCNT composite thin films prepared by sol-gel method on glass substrates have been investigated as a function of MWCNT ratio. The XRD results showed a typical hexagonal wurtzite for AZO:MWCNT thin films with the MWCNT ratio below 0.3 wt.%. The film crystallinity deteriorated with the increasing MWCNT ratio. The sheet resistance of the film decreased from 1.38×10^4 to 10.5 $\Omega/\square$ and the average visible transmittance decreased from 88.5% to 12.1% with the increasing MWCNT ratio from 0 wt.% to 1.0 wt.%. The AZO thin film incorporated with 0.01 wt.% MWCNT possessed the highest figure of merit value ($8 \times 10^{-5}\ \Omega^{-1}$) and was suitable for transparent conducting thin film application.

References

1. T. Minami, T. Miyata, Thin Solid Films 517 (2008) 1474-1477.
2. A.V. Moholkar, S.M. Pawar, K.Y. Rajpure, V. Ganesan, C.H. Bhosale, J. Alloys Compd. 464 (2008) 387-392.
3. Y.Z. Zhang, L.H.Wu, H. Li, J.H. Xu, L.Z. Han, B.C.Wang, Z.L. Tuo, E.Q. Xie, J. Alloys Compd. 473 (2009) 319-322.
4. J. Hu, R.G. Gordon, J. Appl. Phys. 71 (1992) 880-890.
5. B.T. Liu, C.H. Hsu, W.H. Wang, J. Taiwan Institute of Chemical Engineers 43 (2012) 147-152.
6. K.E. Lee, M. Wang, E.J. Kim, S.H. Hahn, Curr. Appl. Phys. 9 (2009) 683-687.
7. F.H. Wang, H.P. Chang, C.C. Tseng, C.C. Huang, Surf. Coat. Technol., 205 (2011) 5269-5277.
8. M.E. Spotnitz, D. Ryan, H.A. Stone, J. Mater. Chem. 14 (2004) 1299-1302.
9. T.V. Sreekumar, T. Liu, S. Kumar, Chem. Mater. 15 (2003) 175-178.
10. M.A. Meitl, Y.X. Zhou, A. Gaur, S. Jeon, M.L. Usrey, M.S. Strano, J.A. Rogers, Nano Lett. 4 (2004) 1643-1647.
11. N.F. Anglada, M. Kaempgen, V. Skakalova, U.D. Weglikowska, S. Roth, Diam. Relat. Mater. 13 (2004) 256-260.
12. L. Hu, D.S. Hecht, G. GrUner, Nano Lett. 4 (2004) 2513-2517.
13. D.H. Zhang, K. Ryu, X.L. Liu, E. Polikarpov, J. Ly, M.E. Tompson, C.W. Zhou, Nano Lett. 6 (2006) 1880-1886.
14. H.Z. Geng, K.K. Kim, K.P. So, Y.S. Lee, Y.K. Chang, Y.H.L.J. Am, Chem. Soc. 129 (2007) 7758-7759.
15. H. Tantang, J.Y. Ong, C.L. Loh, X.C. Dong, P. Chen, Y. Chen, X. Hu, L.P. Tan, L. Li, Carbon 47 (2009) 1867-1885.
16. H. Erismis, D. Nemec, M. Geiss, V. Skakalova, U. Ritter, I. Kolaric, S. Roth, Microelectron. Eng. 88 (2011) 2513-2515.
17. L. Vaisman, H.D. Wagner, G. Marom, Adv. Colloid Interface Sci. 128-130 (2006) 37-46.
18. P.E. Lyons, S. De, F. Blighe, V. Nicolosi, L.F.C. Pereira, M.S. Ferreira, J.N. Coleman, J. Appl. Phys. 104 (2008) 044-302.
19. S. Mandal, R.K. Singha, A. Dhar, S.K. Ray, Mater. Res. Bull. 43 (2008) 244-250.
20. O. Hamad, G. Braunstein, H. Patil, N. Dhere, Thin Solid Films 489 (2005) 303-309.
21. E. Burstein, Phys. Rev. 93 (1954) 632-633.
22. G. Haacke, J. Appl. Phys. 47 (1976) 4086-4089.